Exploring Magneto-Meteorology with Ultra-Hot Jupiters Phase Curves from TESS

Brian Jackson[1*], A. W. Hindle[2], T. M. Rogers[2,3], & E. R. Adams[3]

*bjackson@boisestate.edu; [1]Boise State; [2]Newcastle University; [3]Planetary Science Inst.

The Highlights

- Phase curves for ultra-hot Jupiters are shaped both by the hydrodynamic forces that usually act in planetary atmospheres but also by the planet's magnetic fields, giving rise to a new phenomenon **magneteorology**.
- Magneteorological effects can inhibit equatorial jets, driving the hottest (and brightest) point in the atmosphere westward of the sub-stellar point.
- Competition between magnetic and hydrodynamic forces can results in phase curve oscillations that may be seen in data from the Kepler and TESS missions.

Phase curves for ultra-hot Jupiters show significant variability over tens of days.

Exoplanetary phase curves, light reflected and emitted by the planet as it orbits its star, have revealed exotic weather on these distant worlds. Blistering temperatures on the cloudless daysides of ultra-hot Jupiters partially ionize the atmospheres, allowing them to feel the planets' magnetic fields. Eddy transport of angular momentum within the atmosphere can produce an equatorial jet, while magnetic stresses contribute retrograde accelerations. The competition between these forces can drive the hottest region in the atmosphere back and forth across the sub-stellar point, producing an oscillatory phase curve for some planets.
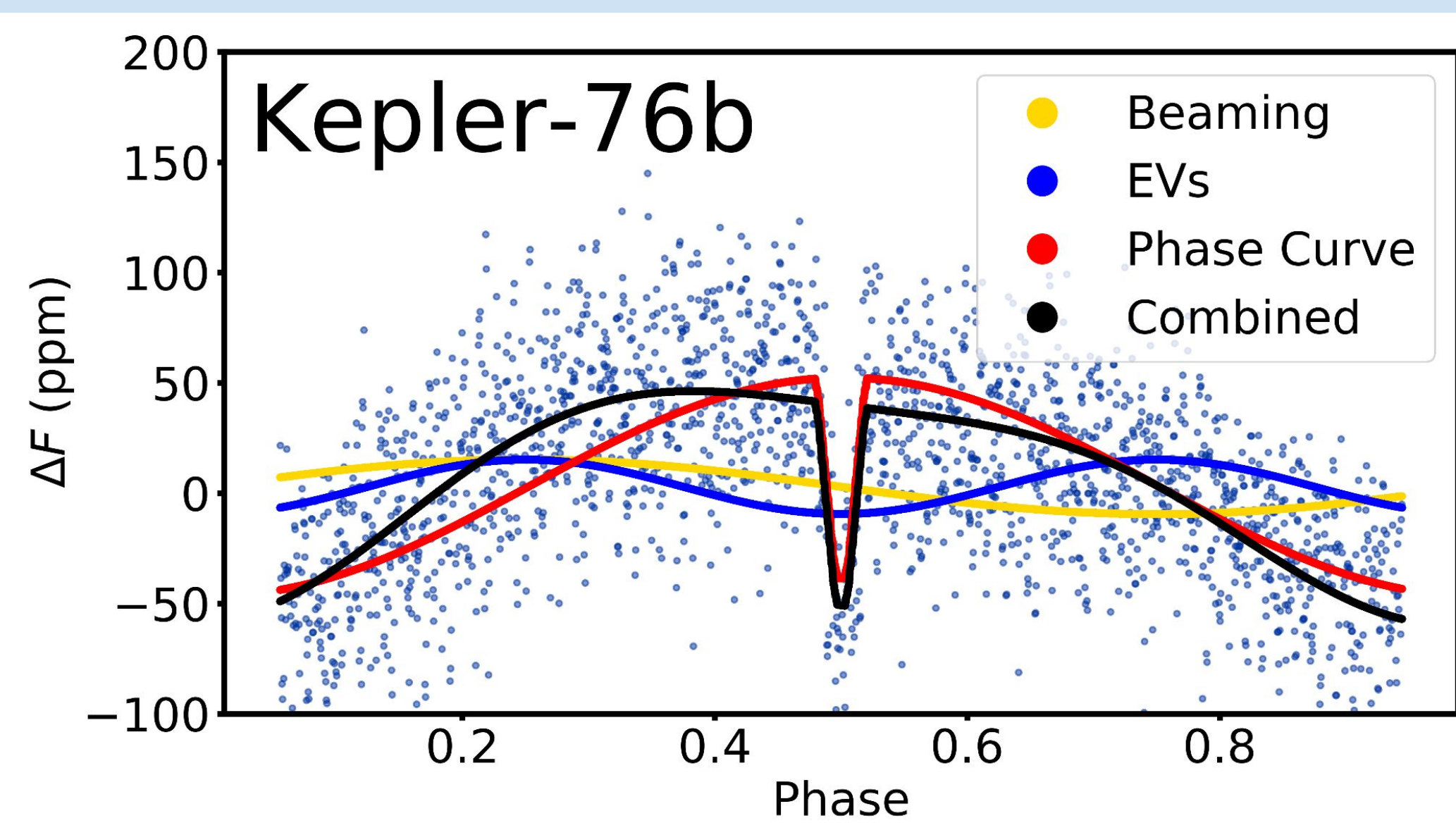

Figure 1. The phase curve (red curve), ellipsoidal variations (blue), beaming signal (yellow), and their combination (black) for the ultra-hot Jupiter Kepler-76 b, a two Jupiter-mass planet with an orbital period of 1.5 days around a 6300-K star. Blue dots show all available observations, conditioned and folded on the ephemeris, with secondary eclipse at 0.5 (primary transit extends below the plot). From Jackson et al. (2019).
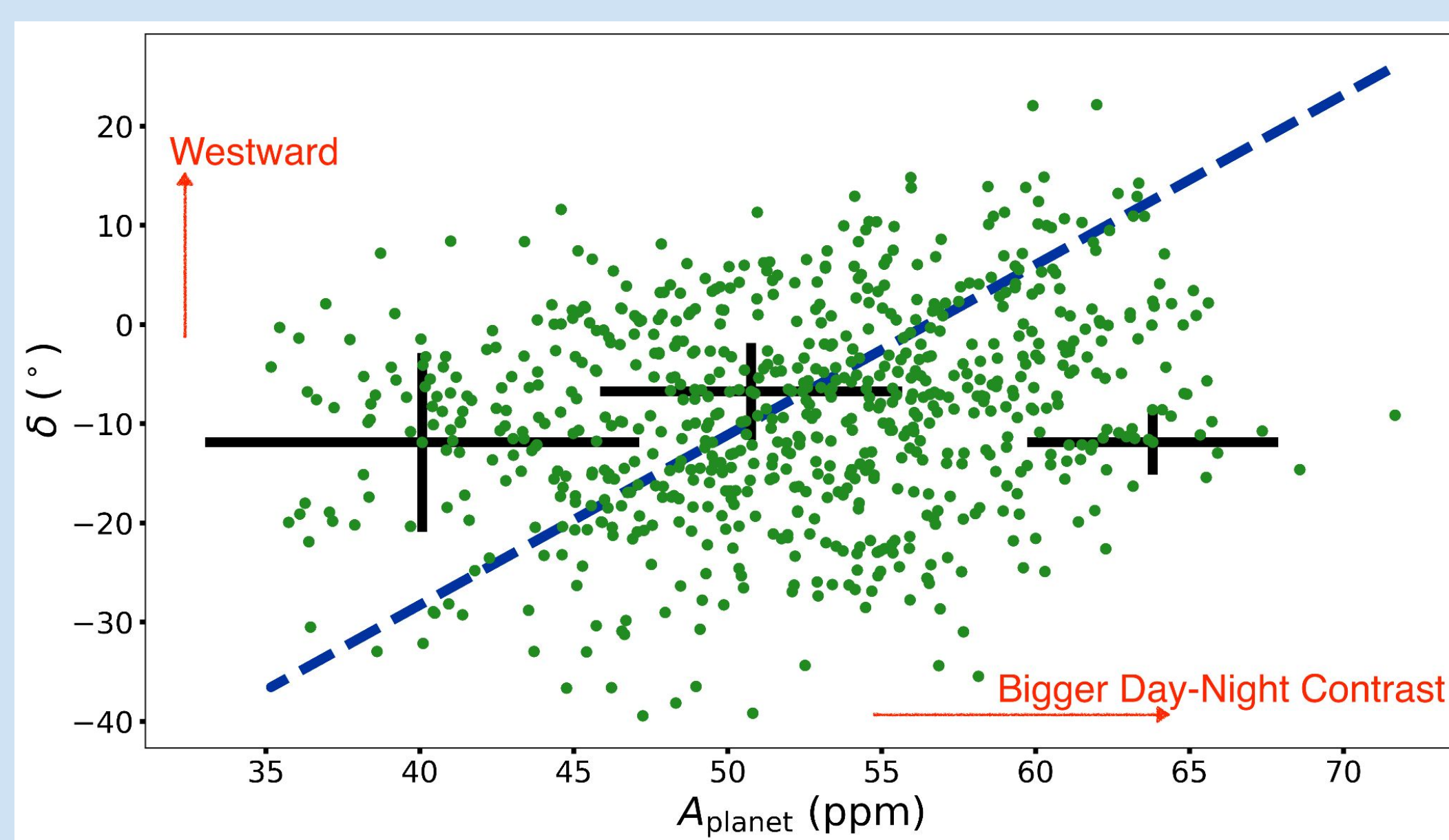

Figure 2. The green points show variations in Kepler-76 b's phase curve amplitude A_{planet} and the angular offset of its peak δ from the substellar point. Jackson et al. (2019) reported a robust positive correlation between A_{planet} and δ which might be expected from magneto-hydrodynamic models: as magnetic forces retard and even reverse the equatorial jet, the dayside will brighten and the phase curve peak will shift west.

Planetary magnetic fields can shape phase curves and drive variability.
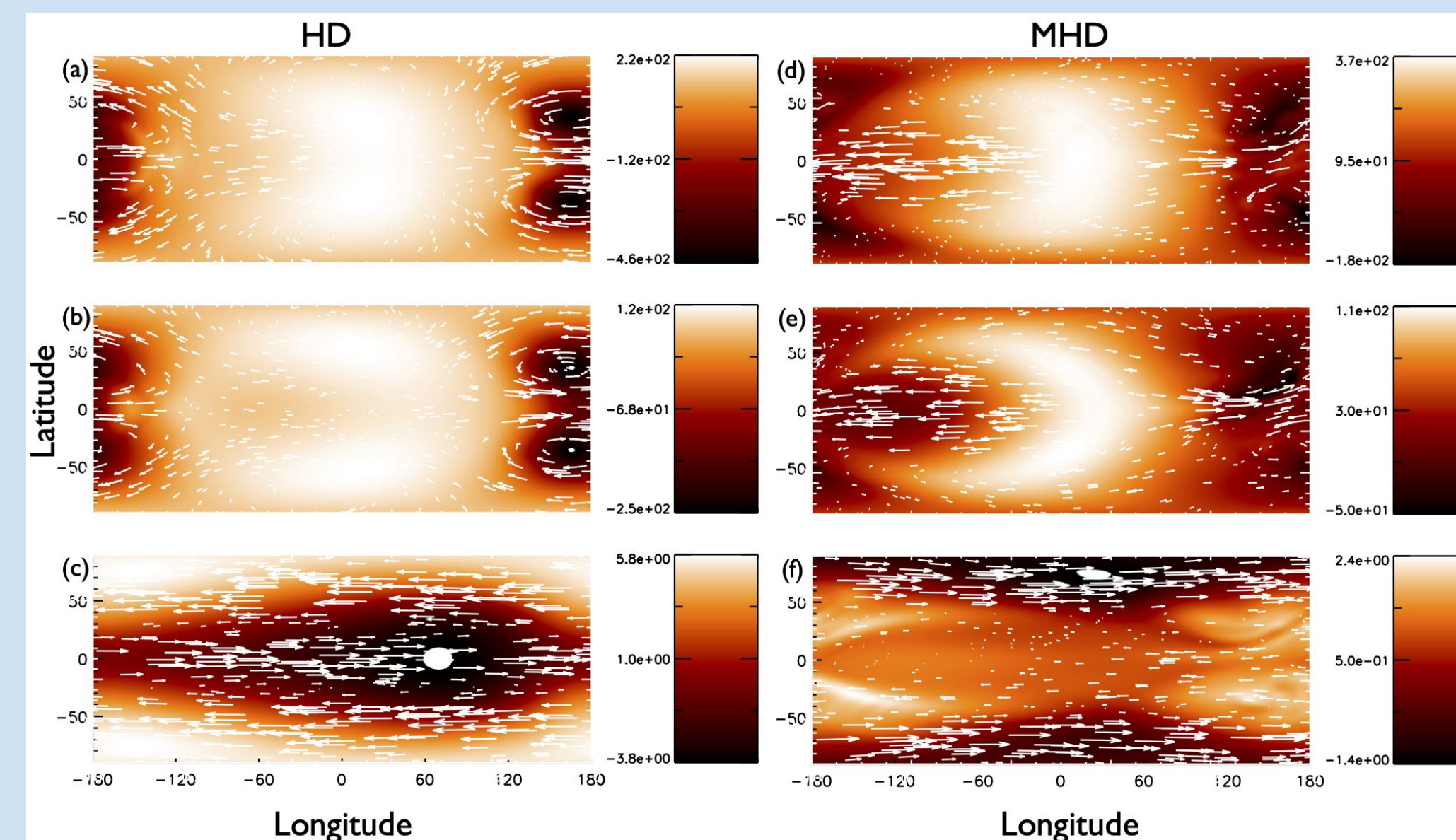

Figure 3. Model temperature perturbations (K), shown in color, and winds, shown with arrows as a function of longitude and latitude at 10 mbar (a,d), 70 mbar (b,e) and 10 bar (c,f). The left column shows results without inclusion magnetic effects, while the right column includes them. From Rogers & Komacek (2014).

See also Hindle et al. (2021) and Hindle's talk in the ultra-short-period planets session on Wednesday.
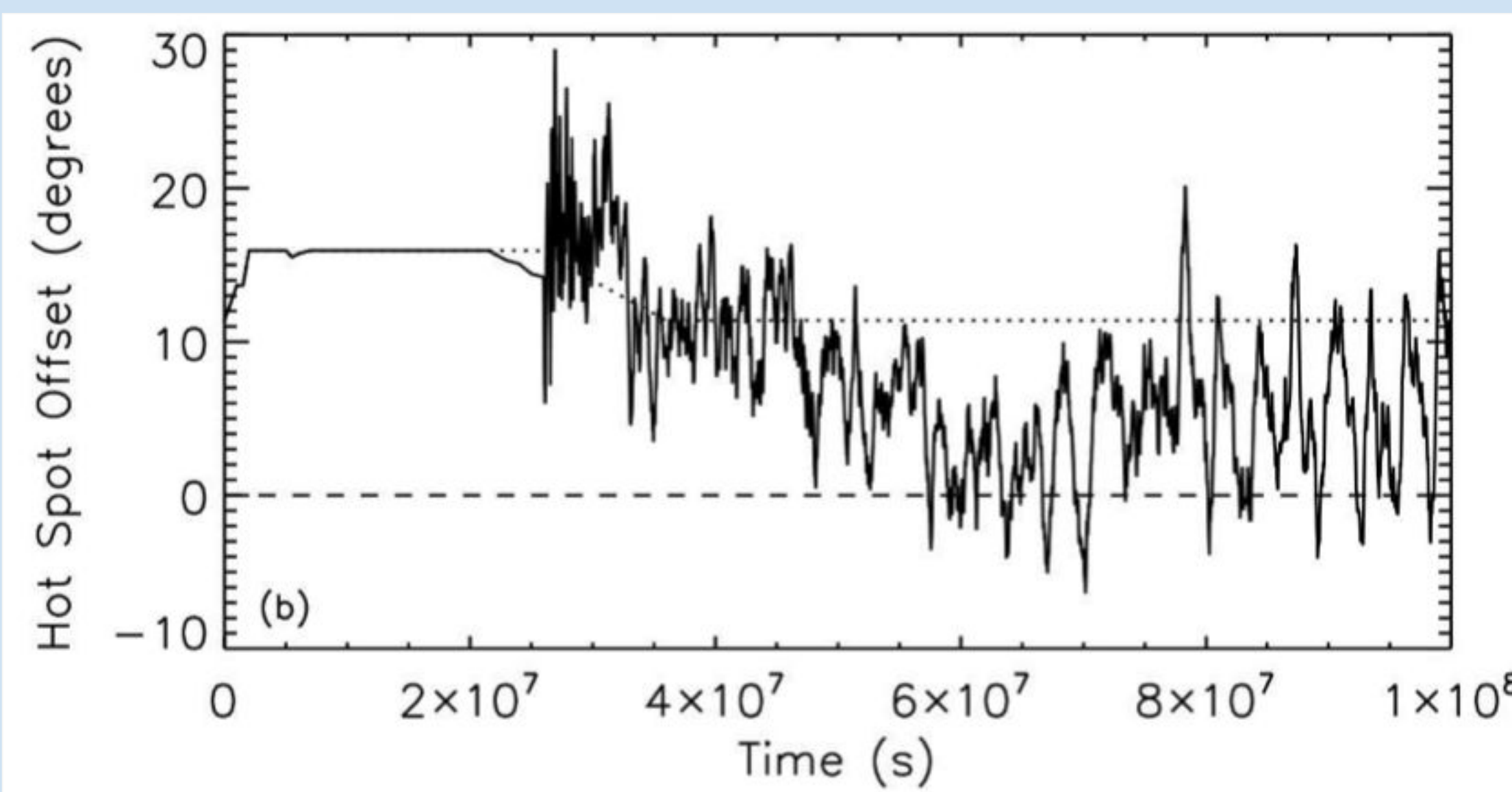

Figure 4. Predicted variability in the offset in the phase curve peak from the sub-stellar point (0 degrees) for HAT-P-7 b. (In contrast to Figure 2, negative offset values in this figure represent westward offsets.) From Rogers (2017).

Kepler-13A b may be an ideal candidate to analyze for phase curve variability.

Discovered and confirmed among the first several Kepler candidates (Faigler & Mazeh 2011, Shporer et al. 2011), Kepler-13A b is a nearly 10-Jupiter mass object in a 1.8-day orbit around a 7700-K, 9.95-magnitude A-star. With a dayside temperature approaching 2800 K and a radius about twice Jupiter's, the object induces a very deep transit and high signal-to-noise phase curve and ellipsoidal variation signals in both Kepler and TESS data. This high SNR makes Kepler-13A b an ideal candidate to search for variability.
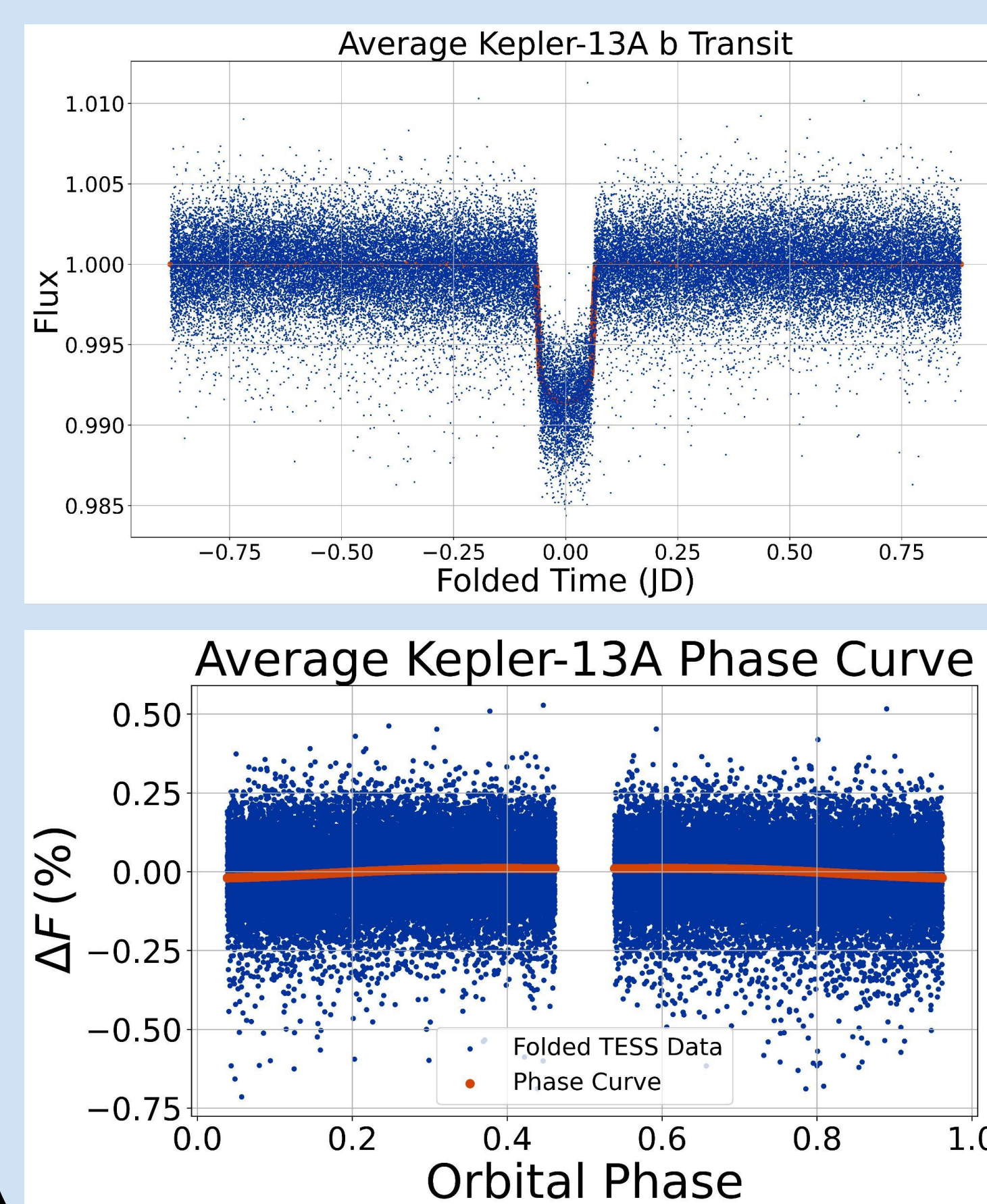

Figure 5. (Top) Sectors 14, 15, and 26 TESS observations of Kepler-13A b folded on the object's orbital period (blue dots). The orange line shows a transit curve. (Bottom) The out-of-transit signals for the same dataset including the planet's phase curve and the ellipsoidal variations. Both the transit and the other light curve use parameters reported in Wong et al. (2021). The planet's phase curve amplitude $A_{planet} = 151 \pm 16$ ppm.

Preliminary analysis of the Kepler-13A b TESS observations show hints of phase curve variability.
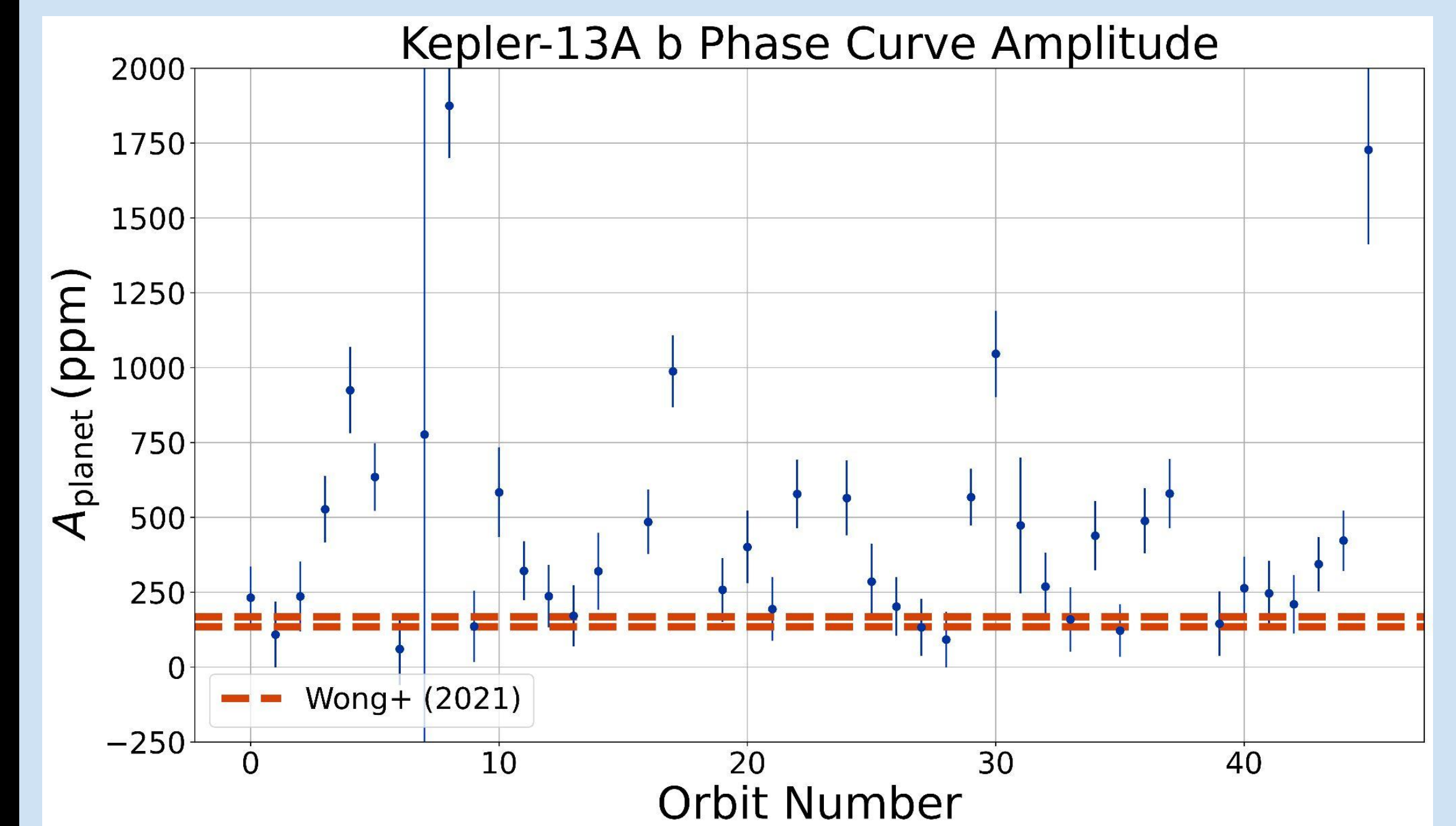

Figure 6. The phase curve amplitudes estimated for the TESS observations of Kepler-13A b, divided up orbit by orbit (blue dots) along with error bars. The dashed, orange lines shows the range of phase curve amplitude for the folded dataset (Figure 5). These results derive from a Levenberg-Marquardt fit of sinusoidal signals.
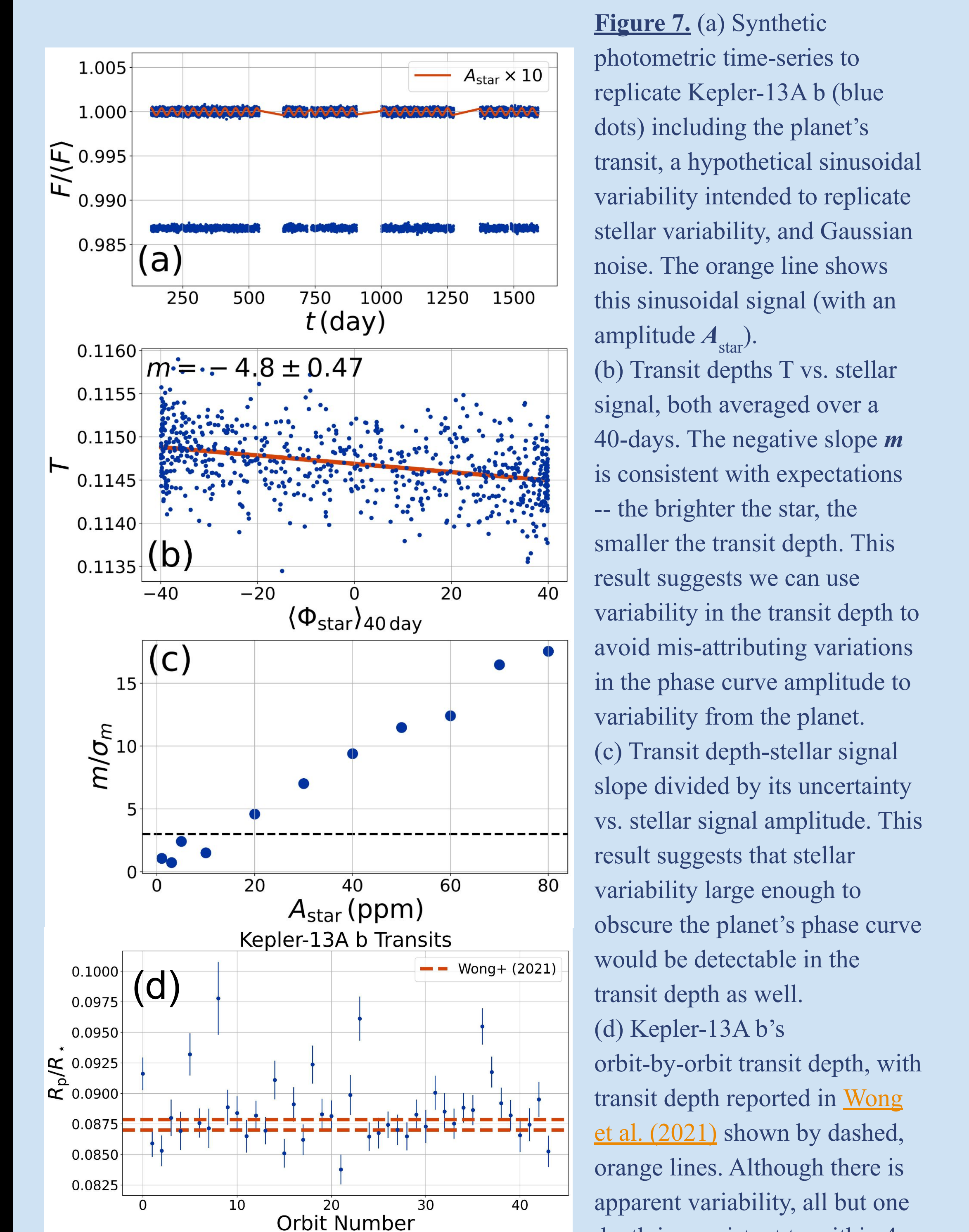

Figure 7. (a) Synthetic photometric time-series to replicate Kepler-13A b (blue dots) including the planet's transit, a hypothetical sinusoidal variability intended to replicate stellar variability, and Gaussian noise. The orange line shows this sinusoidal signal (with an amplitude A_{star}).
(b) Transit depths T vs. stellar signal, both averaged over a 40-days. The negative slope m is consistent with expectations -- the brighter the star, the smaller the transit depth. This result suggests we can use variability in the transit depth to avoid mis-attributing variations in the phase curve amplitude to variability from the planet.
(c) Transit depth-stellar signal slope divided by its uncertainty vs. stellar signal amplitude. This result suggests that stellar variability large enough to obscure the planet's phase curve would be detectable in the transit depth as well.
(d) Kepler-13A b's orbit-by-orbit transit depth, with transit depth reported in Wong et al. (2021) shown by dashed, orange lines. Although there is apparent variability, all but one depth is consistent to within 4-σ.

References

- Jackson, B. et al. (2019) AJ 57(6):239.
- Rogers, T. & Komacek, T. (2014) ApJ 794(2):132.
- Hindle, A. et al. (2021) arXiv:2107.07515.
- Rogers, T. (2017) Nature Astronomy 1:0131.
- Faigler, S. & Mazeh, T. (2011) MNRAS 415, 3921.
- Shporer, A. et al. (2011) AJ 142, 6.
- Wong, I. et al. (2021) arXiv:2106.02610.